Discovery and Investigation of Antiproliferative and Apoptosis-Inducing Properties of New Heterocyclic Podophyllotoxin Analogues Accessible by a One-Step Multicomponent Synthesis

Igor V. Magedov,*[,†,||] Madhuri Manpadi,[‡] Severine Van slambrouck,[‡] Wim F. A. Steelant,[‡] Elena Rozhkova,[†] Nikolai M. Przheval'skii,[†] Snezna Rogelj,[§] and Alexander Kornienko*[,‡]

Department of Organic Chemistry, Timiryazev Agriculture Academy, Moscow 127550, Russia, Department of Chemistry and Department of Biology, New Mexico Institute of Mining and Technology, Socorro, New Mexico 87801, and Intelbioscan Limited, Timiryazevsky Proesd 2, Moscow 127550, Russia

Received May 5, 2007

Podophyllotoxin has been extensively used as a lead agent in the development of new anticancer drugs. On the basis of the previously reported simplified 4-aza-2,3-didehydro podophyllotoxin analogues, we implemented a bioisosteric replacement of the methylenedioxybenzene subunit with a pyrazole moiety to afford tetracyclic dihydropyridopyrazoles. Libraries of these structurally simple analogues are prepared by a straightforward one-step multicomponent synthesis and demonstrated to display antiproliferative properties in a number of human cancer cell lines. These new heterocycles potently induce apoptosis in cancerous Jurkat cells even after a short 24 h exposure. In contrast, no apoptosis is detected in primary lymphocytes under the same treatment conditions. The ease of synthesis and encouraging biological activities make the presented library of dihydropyridopyrazoles promising new leads in anticancer drug design.

Introduction

Natural products and their derivatives have historically been a major source of new pharmaceuticals. According to the analysis of Newman and co-workers, 42% of all drugs approved from 1983 to 1994 originated from natural products.[1] Their role in the drug discovery process is especially pronounced in the areas of anticancer and infectious disease agents, where the fractions of the drugs derived from natural products amount to 60 and 75%, respectively. Because in the process of their biosynthesis natural products interact with many biological macromolecules, they may be considered as evolutionarily selected "privileged structures" that are likely to manifest multiple biological activities.[2,3] Thus, it has been well established that the hit rates obtained by screening of natural product-derived collections of compounds are dramatically higher than those resulting from high throughput screens of combinatorial libraries.[4] This realization has spurred intense research effort aimed at generating natural product-based or natural product-like libraries of compounds in search for new medicinal leads.[5−7]

In a recent review, Feher and Schmidt examined the differences between natural products, commercial drugs, and combinatorial libraries.[8] They found that due to various acyclic and cyclic conformational constraints natural products are in general more rigid, leading to reduced entropic cost of binding and improved oral bioavailability. At the same time, their structures are more complex involving intricate ring systems and larger numbers of stereogenic centers. Therefore, the preparation of natural product-based libraries inevitably involves more sophisticated and laborious synthetic sequences. One way to address this problem is to identify the basic substructure critical for the desired biological activity through SAR[a] studies and, subsequently, simplify the overall structure of the natural product. Therefore, application of MCRs to the construction of natural product-based libraries would be most beneficial to this area of research. Such processes in which three or more reactants are combined together in a single reaction flask to generate a product incorporating most of the atoms contained in the starting materials have the advantages of the intrinsic atom economy, simpler procedures and equipment, time and energy savings, as well as environmental friendliness.[9−14] Despite the extensive use of MCR approaches for the preparation of medicinal libraries,[15] their use in natural product chemistry is rare. The elegant application of the Ugi four-component reaction to the one-step synthesis of cytotoxic aspergillamides and their analogues by Dömling and co-workers is one of the few exceptions, and it serves as a good illustration of how streamlined the preparation of natural product-based libraries can be made with the use of MCRs (Figure 1).[16,17]

Podophyllotoxin (**1**, Figure 2), an antimitotic cyclolignan isolated from plants of the genus *Podophyllum*, was extensively investigated as an antitumor agent, but clinical results were disappointing due to severe gastrointestinal side effects.[18] However, its use as a lead agent in the development of new anticancer drugs has led to the discovery of semisynthetic derivatives, etoposide (**2**) and etoposide phosphate, which are currently used in clinic for the treatment of a variety of malignancies including lung and testicular cancers, lymphoma, nonlymphocytic leukemia, and glioblastoma multiforme.[19] Another agent, teniposide, also prepared by semisynthesis from **1**, is important for the treatment of childhood acute lymphocytic

* Corresponding authors. (A.K.) Phone: +1 505 835 5884. Fax: +1 505 835 5364. E-mail: akornien@nmt.edu. (I.V.M.) Phone: +7 495 976 1639. Fax: +7 495 125 9662. E-mail: intelbioscan@mtu-net.ru.

† Timiryazev Agriculture Academy.

‡ Department of Chemistry, New Mexico Institute of Mining and Technology.

§ Department of Biology, New Mexico Institute of Mining and Technology.

|| Intelbioscan Limited.

[a] Abbreviations: COL, colchicine; DMEM, Dulbecco's modified serum; DMF, dimethylformamide; DMSO, dimethyl sulfoxide; ECL, enhanced chemoluminescence; EDTA, diaminoethanetetraacetic acid; EtOH, ethanol; FBS, fetal bovine serum; FITC, fluorescein isothiocyanate; FOG, Ficoll Orange G; HEPES, 4-(2-hydroxyethyl)-1-piperazinethanesulfonic acid; HHB, Heinz-Hepes buffer; HRMS, high resolution mass spectrometry; MCR, multicomponent reaction; MTT, 3-(4,5-dimethylthazol-2-yl)-2,5-diphenyltetrazolium bromide; PARP, poly(ADP)ribose polymerase; SAR, structure-activity relationships; TLC, thin layer chromatography; RU, relative units; SD, standard deviation; VIN, vinblastine.

10.1021/jm070528f CCC: $37.00
Published on Web 09/26/2007

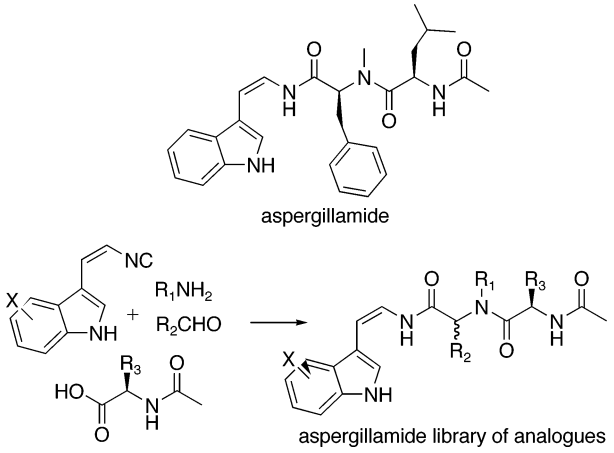

Figure 1. One-step synthesis of aspergillamide-based library of analogues by Ugi four-component reaction.

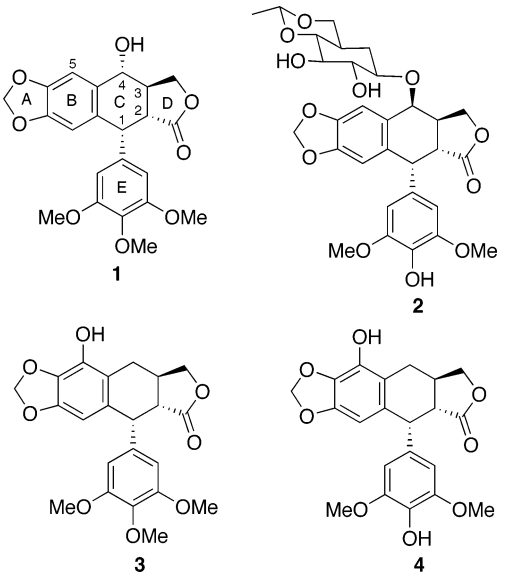

Figure 2. Structures of podophyllotoxin (**1**), etoposide (**2**), *β*-peltatin (**3**), and α-peltatin (**4**).

leukemia.[19] In addition, these agents are used in combination therapies with other drugs. It is noteworthy that unlike **1**, which is a tubulin polymerization inhibitor, **2** is not antimitotic, and it is an inhibitor of DNA topoisomerase II.[20] Because of the development of drug resistance by cancer cells as well as side effects associated with the use of these agents in clinic, which include myelosuppression, neutropenia, and nausea, the search for new effective anticancer drugs with **1** as a lead agent remains an intense area of research.[21,22]

Because of the structural complexity of **1**, arising from the presence of four stereogenic carbons in ring C (Figure 2), most of the SAR studies have been performed by derivatization of the parent natural product rather than by de novo chemical synthesis.[21,22] Such approaches, however, are rather limited by the type of chemistry that **1** can undergo. For example, variations of the ring E are not easy to realize due to the presence of the three methoxy groups in the starting lignan. No matter how laborious, total synthesis efforts are indispensable in this regard. Indeed, Berkowitz and co-workers[23] reported a 19-step synthesis of 3′,4′,5′-tridemethoxy analogue of **1** (ring E = Ph), which is inaccessible by derivatization of the natural product itself.

These issues provide strong impetus to a search for analogues of **1** with drastically simplified structures, which can be accessible via short synthetic sequences from simple starting

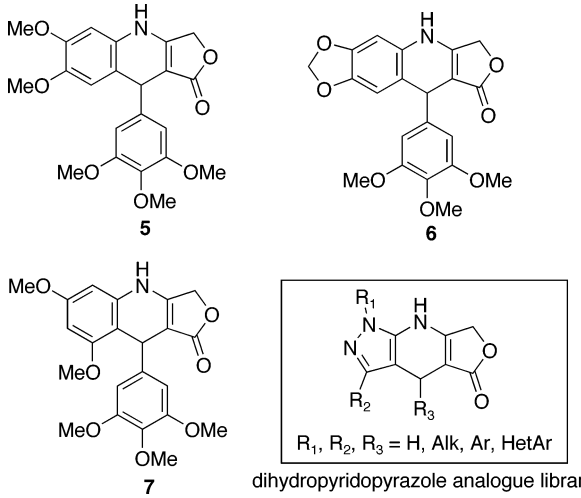

Figure 3. Selected structures of 2,3-didehydro analogues **5**, **6**, and **7** and proposed library of dihydropyridopyrazoles.

materials. Even if such initial compounds might have diminished cytotoxic potencies compared with the parent cyclolignan, the ease of preparation of carefully designed libraries of analogues would lead to more informative SAR studies and expeditious structure optimization. In this connection, Itokawa and Takeya made an important contribution to the field by demonstrating that greatly simplified 4-aza-2,3-didehydropodophyllotoxins **5**−**7** (Figure 3) retain a great fraction of the cytotoxicity associated with the parent lignan.[24,25] Importantly, removal of the stereocenters at C-2 and C-3 solves the problem of epimerization at C-2 that has plagued the clinical development of **1** and its stereochemically complex derivatives, because the rapidly formed in vivo cis-lactone metabolite is significantly less potent.[26] Furthermore, the preparation of such libraries was reduced to a one-step synthesis when Giorgi-Renault and Husson disclosed an MCR leading to these promising anticancer drug leads.[27]

Inspection of the extensive published SAR data of analogues of **1**[21,22] reveals that the intact ring A is not essential for antimitotic activity. In addition, the hydroxyl at C-4 can be repositioned to C-5 leading to the structural type of α- and *β*-peltatins, also isolated from *Podophyllum* plants (**3** and **4** in Figure 2). Although the latter natural products have potent antitumor activity, their severe toxicity resulted in unacceptable clinical trial outcomes.[28,29] Furthermore, phenolic hydroxyl commonly reduces drug bioavailability by making compounds susceptible to oxidation and glucuronidation, and this problem is often addressed with bioisosteric replacement of the phenolic ring with nitrogen-containing heterocycles, such as pyrazoles and triazoles.[30,31] This line of reasoning, together with the success of a structural simplification exemplified by dihydropyridines **5**, **6**, and **7**, has led us to explore dihydropyridopyrazole (Figure 3) analogues of **1**. This novel heterocyclic scaffold represents a most significant structural departure from the natural lead compound. In this article, we disclose a one-step multicomponent synthesis, antiproliferative and apoptosis-inducing properties as well as SAR investigation of the first library of these heterocyclic analogues of **1**.[32]

Results and Discussion

To streamline the preparation of the proposed dihydropyridopyrazoles, we devised a multicomponent route involving the condensation of substituted 5-amino-pyrazoles, tetronic acid, and 3,4,5-trimethoxybenzaldehyde (Figure 4). Since such MCR had been previously investigated using dimedone as a 1,3-dicarbonyl

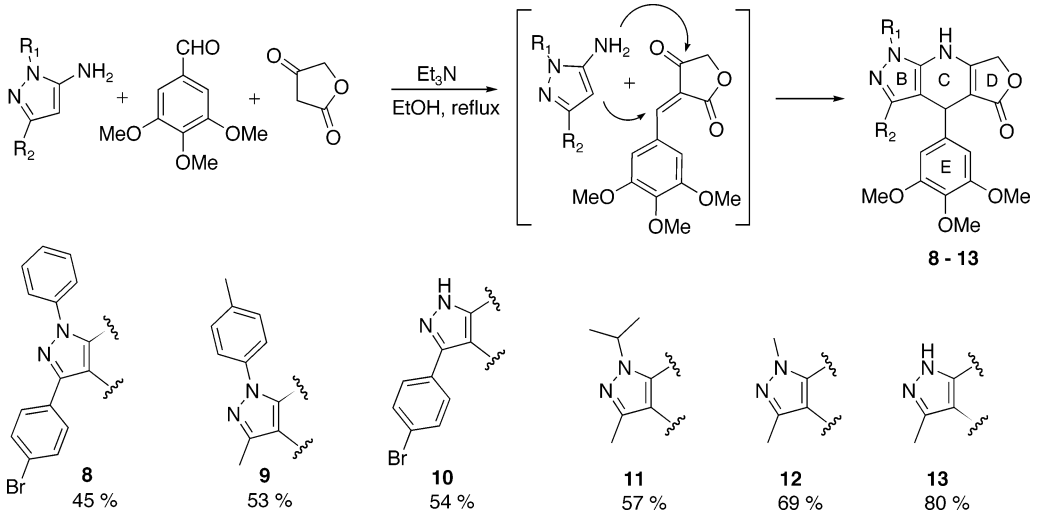

Figure 4. Multicomponent synthesis of dihydropyridopyrazoles with variations in the pyrazole subunit.

component and found to proceed smoothly in refluxing ethanol,[33,34] we employed similar conditions with a single modification involving the addition of triethylamine to shorten the reaction times and improve product yields. This result likely stems from the more facile formation of the intermediate Knoevenagel adduct (Figure 4). In all cases, the resulting dihydropyridopyrazoles precipitate as the reaction mixtures are allowed to cool to room temperature and are isolated by simple filtration. In most cases, no further purification is required because the products are >98% pure as judged by NMR analysis. Various alkyl- and aryl-substituted 5-aminopyrazoles have been reacted to give moderate to good yields of the desired products (Figure 4).

Analogues **8**−**13** were evaluated for antiproliferative activity against three cancer cell lines, HeLa, MCF-7/AZ, and Jurkat as models for human cervical and breast adenocarcinomas and T-cell leukemia, respectively. The corresponding cells were treated with the test compounds at final concentrations of 5 and 50 μM for 48 h, and cell viability was assessed through measurements of mitochondrial dehydrogenase activities using MTT method.[35] The 5 μM data, including those of **1**, **2**, **5**, **6**, and **7** are shown in Table 1.[36] In addition, the same compounds were tested for their ability to induce apoptosis in Jurkat cells in a flow cytometric Annexin-V/propidium iodide assay[37] at final concentrations of 5 μM, and the percentages of apoptotic cells after 48 h of treatment are shown in the last column of Table 1.

The analysis of the data indicates the superior antiproliferative properties of **1** and good potencies of 4-aza-2,3-didehydropodophyllotoxins **5**, **6**, and **7** developed by Itokawa and Takeya.[24,25] **2** is not effective at this concentration; however, its potency is much higher at 50 μM (last row in Table 1) especially against HeLa cells. Among the pyrazole analogues, compound **13** shows very similar potencies and activity profiles to compounds **5**, **6**, and **7**, suggesting that the alkoxybenzene ring can be replaced by the pyrazole moiety without loss of potency. Because the growth inhibitory activity is much less pronounced with analogues possessing larger substituents on the pyrazole ring (**8**−**11**) or the methylated pyrazole nitrogen (**12** versus **13**), the pyrazole moiety of analogue **13** appeared optimal for further investigation. In addition, the magnitudes of apoptosis observed in the Jurkat cell line are similar for **1**, **5**, **6**, **7**, **13** (at 5 μM), and **2** (at 50 μM), amounting to 50−55%.

Next, a library of ring E analogues **14**−**40**, based on the pyrazole subunit of compound **13**, was obtained by condensation of 5-amino-3-methylpyrazole, tetronic acid, and various aromatic, heteroaromatic, and aliphatic aldehydes. The yields of the synthesized dihydropyridopyrazoles, their antiproliferative potencies against the same three cell lines, and percent of apoptosis induction of Jurkat cells are given in Table 2.

Table 1. Optimization of the Pyrazole Moiety of the Dihydropyridopyrazole Structure[a]

	% cell viability[b]			
compound	HeLa	MCF-7/AZ	Jurkat	% apoptosis[c] Jurkat
1	19 ± 5	55 ± 3	18 ± 5	54 ± 2
2	91 ± 2	76 ± 2	75 ± 5	4 ± 3
5	53 ± 5	58 ± 4	35 ± 6	49 ± 4
6	54 ± 6	52 ± 3	54 ± 1	55 ± 4
7	55 ± 2	43 ± 2	55 ± 4	55 ± 4
8	73 ± 5	90 ± 3	99 ± 1	2 ± 1
9	77 ± 4	71 ± 5	77 ± 2	23 ± 1
10	67 ± 4	98 ± 3	78 ± 7	5 ± 1
11	83 ± 5	99 ± 0	77 ± 9	4 ± 0
12	55 ± 3	98 ± 1	79 ± 4	5 ± 1
13	50 ± 2	58 ± 5	47 ± 3	55 ± 4
2 at 50 μM	15 ± 3	57 ± 4	50 ± 2	61 ± 6

[a] Antiproliferative and apoptosis-inducing properties of compounds **8**−**13** relative to literature control agents. [b]Percent of remaining cell viability after 48 h of treatment with indicated compounds at the final concentration of 5 μM relative to DMSO control ±SD from two independent experiments, each performed in eight replicates. Determined by MTT assay. [c]Percent of apoptotic cells after 48 h of treatment with indicated compounds at the final concentration of 5 μM relative to DMSO control ±SD from two independent experiments, each performed in three replicates. Determined by flow cytometric Annexin-V/propidium iodide assay.

The examination of the data shows that in addition to the potent antiproliferative and apoptosis-inducing properties of analogue **13**, possessing the podophyllotoxin-like trimethoxy ring E, all of the other most potent analogues, namely **21**−**26**, have a bromine substituent at the meta position of the aromatic ring E. Intriguingly, this preference remains unchanged whether there are other substituents at positions C4′ and C5′of the ring E. Thus, H (**21**), OH, Br (**22**), OMe, OEt (**23**, **24**, **26**), OAc (**24**), or NMe_2 (**25**) groups are well tolerated. *m*-Cl (**27**, **28**), *m*-F (**29**) substituents, or ortho (**30**) and para (**31**) positioning of the bromine do not produce an effect similar to the meta bromo substituent. Heterocyclic analogues (**34**−**40**) are much less potent or inactive. In general, percent of apoptosis induction in Jurkat cells parallels the antiproliferative potency of the analogues being highest (50−58%) with the meta bromo analogues **21**−**26**.

Table 2. Optimization of the Ring E Structure (Antiproliferative and Apoptosis-Inducing Properties of Compounds **14**−**40**)

compound	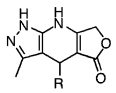 R	Synthesis % yield	% cell viability[a]			% apoptosis[b] Jurkat
			HeLa	MCF-7/AZ	Jurkat	
14	3,4-*di*-MeO-Ph	82	73 ± 3	95 ± 4	88 ± 2	5 ± 1
15	4-MeO-Ph	72	73 ± 7	82 ± 3	94 ± 4	11 ± 1
16	4-F_3CO-Ph	67	97 ± 2	84 ± 3	97 ± 6	9 ± 2
17	4-MeS-Ph	79	45 ± 2	95 ± 4	87 ± 4	14 ± 6
18	Ph	83	74 ± 4	84 ± 3	87 ± 5	10 ± 2
19	2-O_2N-Ph	47	71 ± 4	99 ± 2	64 ± 1	6 ± 1
20	4-HO-3-MeO-5-O_2N-Ph	76	78 ± 3	89 ± 5	90 ± 2	5 ± 1
21	3-Br-Ph	76	51 ± 3	63 ± 4	68 ± 3	58 ± 2
22	3,5-*di*-Br-4-HO-Ph	52	58 ± 7	60 ± 4	58 ± 3	53 ± 0
23	3-Br-4-EtO-5-MeO-Ph	76	52 ± 2	49 ± 4	28 ± 5	49 ± 1
24	4-AcO-3-Br-5-MeO-Ph	73	47 ± 2	46 ± 2	36 ± 6	58 ± 1
25	3-Br-4-Me_2N-Ph	75	55 ± 3	59 ± 3	34 ± 5	41 ± 1
26	3-Br-4,5-*di*-MeO-Ph	78	16 ± 3	47 ± 1	29 ± 3	56 ± 1
27	3-Cl-Ph	78	43 ± 4	54 ± 3	76 ± 4	28 ± 4
28	3,4-*di*-Cl-Ph	75	88 ± 1	56 ± 3	71 ± 4	33 ± 4
29	3-F-Ph	63	99 ± 1	76 ± 2	84 ± 2	28 ± 1
30	2-Br-Ph	58	57 ± 4	100 ± 3	90 ± 1	8 ± 2
31	4-Br-Ph	83	62 ± 3	92 ± 2	90 ± 1	10 ± 2
32	Me	37	70 ± 4	97 ± 2	78 ± 5	5 ± 1
33	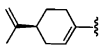	54	95 ± 5	91 ± 4	89 ± 6	14 ± 2
34		61	58 ± 2	100 ± 1	94 ± 2	6 ± 1
35		84	82 ± 4	98 ± 3	74 ± 4	18 ± 1
36		92	98 ± 2	100 ± 2	82 ± 5	6 ± 4
37		55	94 ± 1	100 ± 1	92 ± 5	4 ± 2
38		59	69 ± 4	96 ± 2	88 ± 9	11 ± 3
39		78	84 ± 4	100 ± 3	85 ± 6	7 ± 2
40	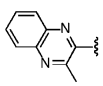	57	72 ± 6	100 ± 4	97 ± 3	11 ± 2

[a] Perecent of remaining cell viability after 48 h of treatment with indicated compounds at the final concentration of 5 μM relative to DMSO control ±SD from two independent experiments, each performed in eight replicates. Determined by MTT assay. [b]Percent of apoptotic cells after 48 h of treatment with indicated compounds at the final concentration of 5 μM relative to DMSO control ±SD from two independent experiments, each performed in three replicates. Determined by flow cytometric Annexin-V/propidium iodide assay.

Morphological changes of cells treated with potent dihydropyridopyrazole analogues can be visually observed with light microscopy (Figure 5). The phenotypic changes, such as formation of fingerlike extensions and shriveling, are observed with adherent (MCF-7/AZ) and suspension (Jurkat) cells, respectively. Furthermore, rounding up and detachment of the

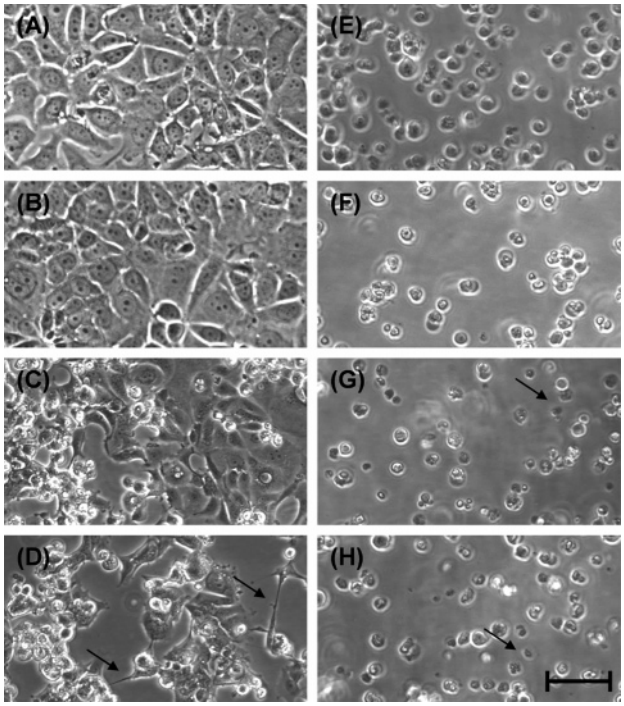

Figure 5. Light microscopy pictures. MCF-7/AZ (A−D) and Jurkat cells (E−H) treated for 0 (A, E), 24 (B, F), 48 (C, G), and 72 h (D, H) with **13** at 5 μM. Treatment of MCF-7/AZ cells with **13** for 48 or 72 h induces formation of finger-like extensions (indicated by arrows), rounding, and detachment (C, D). Treatment of Jurkat cells with **13** for 48 or 72 h induces shriveling (indicated by arrows, G, H). The scale bar indicates 40 μm.

Table 3. Comparative Antiproliferative Potencies Expressed as Concentrations Required for 50% of the Effect

compound	GI_{50} (μM)[a] HeLa	compound	GI_{50} (μM)[a] HeLa	compound	GI_{50} (μM)[a] HeLa
1	0.02	**13**	5 ± 1	**24**	4 ± 1
2	8 ± 2	**21**	5 ± 1	**25**	6 ± 1
5	6 ± 1	**22**	8 ± 2	**26**	0.75 ± 0.1
6	6 ± 1	**23**	5 ± 1	**27**	10 ± 2

[a] Concentration required to reduce the viability of HeLa cells by 50% after 48 h of treatment with indicated compounds relative to DMSO control ±SD from two independent experiments, each performed in eight replicates. Determined by MTT assay.

adherent cells is indicative of extensive cell death occurring in cultures treated with potent library analogues, such as **13** in Figure 5.

To compare the antiproliferative potencies in terms of concentrations required for 50% of the effect, selected analogues were tested in dose-dependent manner against HeLa cell line, and the obtained GI_{50} values are listed in Table 3. The results reveal that dihydropyridopyrazoles (**13**, **21**−**26**) and Itokawa/Takeya's analogues (**5**, **6**) have similar potencies, possessing GI_{50} values in low micromolar range, while analogue **26** stands out as a submicromolar compound. All meta bromo analogues have slightly lower GI_{50} values than that of **2** but 35−400 times higher than that of **1**.

An important biochemical change that takes place in cells undergoing apoptosis is flipping of phosphatidylserine lipid from the inner leaflet of the cellular membrane to the outer one. This event leads to the removal of the apoptotic cells in vivo through their specific recognition by the phagocytes expressing phosphatidylserine-binding anticoagulant protein Annexin V on their cell surface.[38] So far in this work Annexin V conjugate with FITC has been used in the flow cytometric detection and

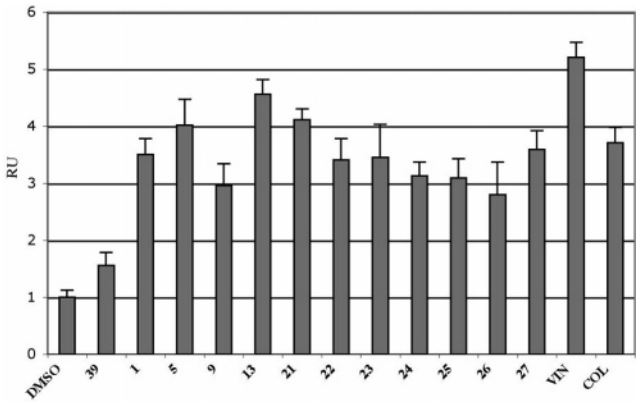

Figure 6. Caspase-3 activation in Jurkat cells with indicated compounds used at 5 μM (VIN was used at 1 μM). The magnitudes of activation are expressed as RU with DMSO control assigned the value of one. Error bars represent data from two independent experiments with each performed in duplicates.

quantification of the fraction cells displaying an increase in fluorescence. It has been reported that the anticancer efficacy of many currently used chemotherapeutic agents is strongly correlated with their ability to induce apoptosis in cancer cells,[39] and therefore many primary screens for novel anticancer leads are now based not on identification of compounds with antiproliferative activity, but rather on their apoptosis-inducing properties.[40−42] Therefore, to obtain further insight into the apoptosis induction effect of the dihydropyridopyrazoles, additional experiments were performed.

Caspases are a family of proteolytic enzymes, which are normally present inside the cells as zymogens, that upon activation during the apoptotic process cleave many protein substrates resulting in irreversible cell death. Among several such proteases in the caspase activation cascade, caspase-3 is one of the most downstream enzymes and it is commonly referred to as an effector caspase. Thus, the compounds that showed apoptosis induction in the Annexin V flow cytometric assay were also evaluated for their ability to induce caspase-3 activation in Jurkat cells (Figure 6). Indeed, analogues **13** and **21**−**27** used at 5 μM concentrations elicited 3 to 4.5 fold increase in caspase-3 activity; these magnitudes are in the similar range with antimitotic agents **1**, colchicine, and the clinically used drug vinblastine. In contrast, compound **39**, which showed little apoptosis induction in the Annexin V assay (7%, Table 2), was similarly ineffective in activating caspase-3 in this cell line.

Apoptosis was further characterized by the Western blot analysis (Figure 7). Cleavage of the procaspase-3 to produce the active enzyme was observed in Jurkat cells in a time-dependent manner after treating the cells with **1** (A), VIN (B), and active analogue **13** (C). The procaspase-3 remained intact over the duration of the experiment when the same cells were treated with inactive analogue **39** (D). In addition, cleavage of PARP, a genome surveillance enzyme and endogenous substrate cleaved by caspases during the apoptotic process, was observed with **1**, VIN, and **13**, but not inactive **39**.

Because endonuclease-mediated cleavage of nuclear DNA resulting in formation of oligonucleosomal DNA fragments (180−200 base pairs long) is a hallmark of apoptosis in many cell types, DNA-laddering assay was performed (Figure 8). Jurkat cells were treated with analogue **13** at different concentrations (lanes B, C, D, E), **2** (lanes F and G duplicate at 50 μM), and DMSO (lane H) for 24 h. After that the cellular DNA was isolated and electrophoresed in a 1.5% agarose gel. The

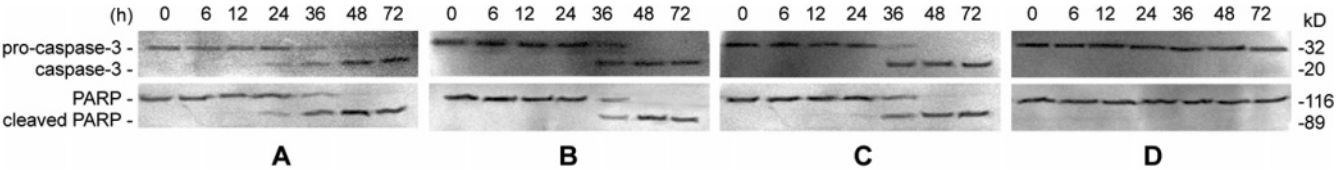

Figure 7. Western blot analysis. Time-dependent effect of **1** (5 μM, A), VIN (1 μM, B), **13** (5 μM, C), and **39** (5 μM, D). Immunostaining of pro-caspase-3 and caspase-3 using anti-caspase-3 chemoluminescent antibody and PARP and its cleavage product using anti-PARP chemoluminescent antibody.

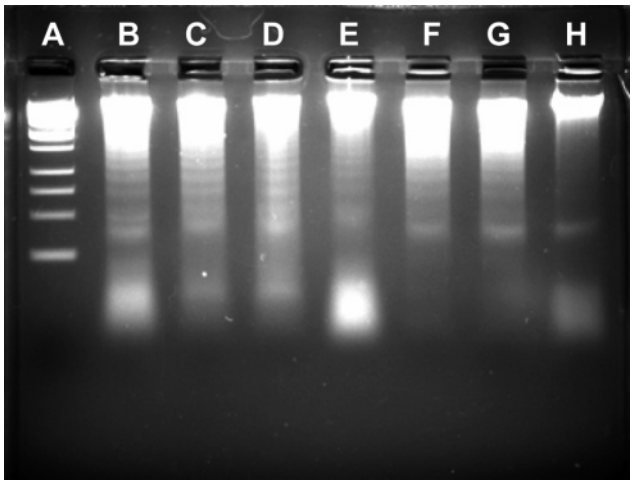

Figure 8. DNA laddering in Jurkat cells after 24 h of treatment. (A) Molecular weight marker, (B) **13** at 50 μM, (C) **13** at 10 μM, (D) **13** at 5 μM, (E) **13** at 1 μM, (F, G) **2** at 50 μM, (H) DMSO control (0.1%).

characteristic ladder pattern was obtained with compound **13** at a concentration as low as 1 μM. **2** displayed a similar effect, while no laddering was observed when the cells were treated with the DMSO control.

Finally, because the normal nucleated white blood cells are a common target of many cancer chemotherapeutic agents leading to such serious side effects as leukopenia and neutropenia, the dihydropyridopyrazole analogues were tested for their ability to induce apoptosis in human primary lymphocytes. Human lymphocytes were purified from whole blood obtained from healthy volunteers and treated with analogues **13**, **21**−**26**, as well as **1** and **2** to assess the extent of apoptosis induction with flow cytometric Annexin-V/propidium iodide assay. Pleasingly, none of these compounds show any apoptosis induction in human noncancerous lymphocytes after 24 h of treatment. This finding stands in sharp contrast with the propensity of these compounds to induce extensive apoptosis in Jurkat cells (data for **1**, **2**, **13**, and **21** are shown in Figure 9).

Conclusions

Itokawa and Takeya have previously shown that drastically simplified 4-aza-2,3-didehydro podophyllotoxin analogues are important new anticancer drug leads because such compounds retain a significant fraction of cytotoxic potency. In this work we further modified the multicyclic core of the natural product by replacing the alkoxy-substituted benzene ring (A, B) with a pyrazole moiety. This resulted in further structural simplification affording tetracyclic dihydropyridopyrazoles. Libraries of these new heterocyclic compounds are accessible by a straightforward one-step multicomponent synthesis, which involves simple isolation of the products by filtration and requires no further purification of library members. The new compounds are comparable in their antiproliferative properties with Itokawa and Takeya's compounds and are slightly more potent than the currently used anticancer drug etoposide. Although the dihydropyridopyrazoles are 35−400 times less potent than podophyllotoxin itself, these magnitudes are quite acceptable given the drastic reduction of structural complexity and possibilities for rapid synthesis of new libraries in search for more potent compounds. Moreover, the new compounds are racemic, and thus the separation and testing of individual enantiomers will undoubtedly lead to more potent compounds. In addition, the ability of dihydropyridopyrazoles to induce apoptosis in Jurkat cells was demonstrated by multiple techniques, and these new compounds are very similar to podophyllotoxin in magnitudes of apoptosis induction. These observations, as well as the fact that the new heterocycles induce virtually no apoptosis in noncancerous-nucleated white blood cells, make the presented library of dihydropyridopyrazoles promising new leads in anticancer drug design. Whether these compounds exert their cytotoxic effect through podophyllotoxin-like antitubulin mechanism, target topoisomerase II, or have a totally independent mode of action constitutes the subject of further investigation, which will be reported in due course.

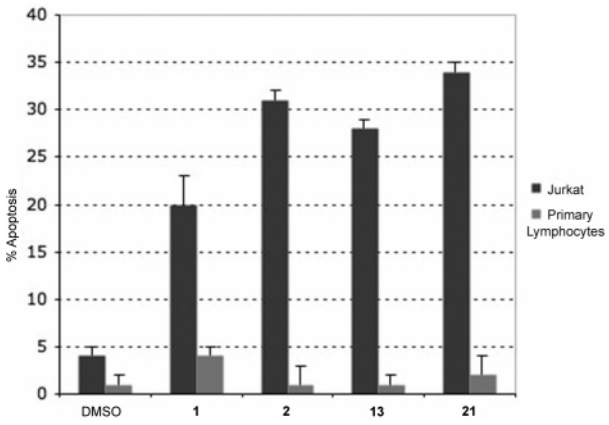

Figure 9. Comparative evaluation of apoptosis-inducing properties of analogues **13** (5 μM) and **21** (5 μM) as well as **1** (5 μM) and **2** (50 μM) in primary lymphocytes and Jurkat cells. Percent of apoptotic cells after 24 h of treatment with indicated compounds at the final concentration of 5 μM and 0.1% DMSO relative to untreated control cells ±SD from two independent experiments, each performed in duplicates. Determined by flow cytometric Annexin-V/propidium iodide assay.

Experimental Section

All aldehydes, aminopyrazoles, and tetronic acid were purchased from commercial sources and used without purification. Triethylamine (Et_3N) was distilled from CaH_2. All reactions were performed in a reaction vessel open to the atmosphere and monitored by thin layer chromatography (TLC) on precoated (250 μm) silica gel $60F_{254}$ glass-backed plates. Visualization was accomplished with UV light and aqueous ceric ammonium molybdate solution or potassium permanganate stain followed by charring on a hot-plate. ^1H and ^{13}C NMR spectra were recorded on JEOL 300 MHz spectrometer. MS analyses were performed at the Mass Spectrometry Facility, University of New Mexico.

General Procedure for Dihydropyridopyrazole Synthesis. A mixture of a substituted 5-amino-pyrazole (1 mmol), tetronic acid

(1 mmol), triethylamine (0.05 mL), and a corresponding aldehyde (1 mmol) in EtOH (4 mL) was refluxed for 0.5−3 h. The reaction mixture was allowed to cool to room temperature, and the precipitated product was collected by vacuum filtration and washed with EtOH (3 mL) at room temperature. In most cases, the products were >98% pure as judged by NMR analysis. When an impurity was present, the product was recrystallized from DMF/H_2O.

4-(3,4,5-Trimethoxyphenyl)-3-(4-bromophenyl)-1-phenyl-1,4,7,8-tetrahydro-5*H*-furo[3,4-*b*]pyrazolo[4,3-*e*]pyridin-5-one (8). ^{1}H NMR (DMSO-d_6, δ): 10.36 (s, 1H), 7.48−7.67 (m, 9H), 6.45 (s, 2H), 5.32 (s, 1H), 4.87 (m, 2H), 3.61 (s, 6H), 3.56 (s, 3H). ^{13}C NMR (DMSO-d_6, δ): 172.1, 158.7, 153.0, 147.8, 140.8, 139.4, 138.1, 136.6, 132.8, 131.7, 130.2, 129.7, 128.5, 124.4, 121.6, 105.9, 102.2, 60.5, 56.3, 35.8. Anal. ($C_{29}H_{24}BrN_3O_5$) C, H, N.

4-(3,4,5-Trimethoxyphenyl)-3-methyl-1-(4-methylphenyl)-1,4,7,8-tetrahydro-5*H*-furo[3,4-*b*]pyrazolo[4,3-*e*]pyridin-5-one (9). ^{1}H NMR (DMSO-d_6, δ): 10.13 (s, 1H), 7.33−7.42 (m, 4H), 6.56 (s, 2H), 4.84 (m, 3H), 3.73 (s, 6H), 3.63 (s, 3H), 2.38 (s, 3H), 1.90 (s, 3H). ^{13}C NMR (DMSO-d_6, δ): 172.1, 159.3, 153.2, 147.1, 141.1, 137.9, 137.3, 136.7, 136.0, 135.5, 130.5, 123.7, 105.0, 103.1, 99.8, 65.7, 60.5, 56.5, 35.7, 21.1, 12.9. HRMS *m*/*z* (ESI) calcd for $C_{25}H_{25}N_3O_5Na$ (M + Na)$^+$, 470.1687; found, 470.1692.

3-(4-Bromophenyl)-4-(3,4,5-trimethoxyphenyl)-1,4,7,8-tetrahydro-5*H*-furo[3,4-*b*]pyrazolo[4,3-*e*]pyridin-5-one (10). ^{1}H NMR (DMSO-d_6, δ): 10.30 (s, 1H), 7.47−7.57 (m, 4H), 6.34 (s, 1H), 5.21 (s, 1H), 4.86 (m, 3H), 3.47 (s, 6H), 3.52 (s, 3H). ^{13}C NMR (DMSO-d_6, δ): 172.3, 152.8, 141.1, 138.3, 136.5, 132.1, 129.4, 105.4, 102.9, 65.2, 60.4, 56.2, 35.2, 19.1. HRMS *m*/*z* (ESI) calcd for $C_{23}H_{20}BrN_3O_5Na$ (M + Na)$^+$, 520.0479; found, 520.0484.

4-(3,4,5-Trimethoxyphenyl)-3-methyl-1-(1-methylethyl)-1,4,7,8-tetrahydro-5*H*-furo[3,4-*b*]pyrazolo[4,3-*e*]pyridin-5-one (11). ^{1}H NMR (DMSO-d_6, δ): 10.31 (s, 1H), 6.44 (s, 2H), 4.88 (m, 3H), 4.38 (m, 1H), 3.64 (m, 9H), 1.81 (s, 3H), 1.33 (m, 6H). ^{13}C NMR (DMSO-d_6, δ): 172.5, 158.9, 153.1, 144.7, 141.4, 137.2, 136.7, 105.7, 101.3, 99.1, 65.6, 60.5, 56.3, 48.8, 35.7, 22.5, 13.2. Anal. ($C_{21}H_{25}N_3O_5$) C, H, N.

4-(3,4,5-Trimethoxyphenyl)-1,3-dimethyl-1,4,7,8-tetrahydro-5*H*-furo[3,4-*b*]pyrazolo[4,3-*e*]pyridin-5-one (12). ^{1}H NMR (DMSO-d_6, δ): 10.42 (s, 1H), 6.47 (s, 2H), 4.90 (m, 3H), 3.69 (s, 6H), 3.61 (m, 6H), 1.77 (s, 1H). ^{13}C NMR (DMSO-d_6, δ): 172.3, 158.8, 153.1, 144.6, 141.3, 136.7, 105.7, 101.4, 99.0, 65.4, 60.5, 56.3, 35.9, 35.1, 12.9. Anal. ($C_{19}H_{21}N_3O_5$) C, H, N.

3-Methyl-4-(3,4,5-trimethoxyphenyl)-1,4,7,8-tetrahydro-5*H*-furo[3,4-*b*]pyrazolo[4,3-*e*]pyridin-5-one (13). ^{1}H NMR (DMSO-d_6, δ): 11.9 (s, 1H), 10.1 (s, 1H), 6.47 (s, 2H), 4.84 (m, 3H), 3.68 (s, 9H), 1.9 (s, 3H). ^{13}C NMR (DMSO-d_6, δ): 172.6, 160.6, 153.1, 147.6, 141.5, 136.7, 136.3, 105.4, 102.8, 96.1, 65.4, 60.5, 56.3, 35.3, 10.3. Anal. ($C_{18}H_{19}N_3O_5$) C, H, N.

3-Methyl-4-(3,4-dimethoxyphenyl)-1,4,7,8-tetrahydro-5*H*-furo-[3,4-*b*]pyrazolo[4,3-*e*]pyridin-5-one (14). ^{1}H NMR (DMSO-d_6, δ): 11.85 (s, 1H), 10.04 (s, 1H), 6.59−6.81 (m, 3H), 4.79 (m, 3H), 3.67 (s, 6H), 1.83 (s, 3H). ^{13}C NMR (DMSO-d_6, δ): 172.7, 160.2, 148.9, 147.6, 138.5, 136.6, 120.1, 112.3, 112.2, 103.2, 96.5, 65.3, 56.01, 34.6, 10.2. HRMS *m*/*z* (ESI) calcd for $C_{17}H_{17}N_3O_4$ (M + Na)$^+$, 350.1126; found, 350.1117.

3-Methyl-4-(4-methoxyphenyl)-1,4,7,8-tetrahydro-5*H*-furo-[3,4-*b*]pyrazolo[4,3-*e*]pyridin-5-one (15). ^{1}H NMR (DMSO-d_6, δ): 11.85 (s, 1H), 10.04 (s, 1H), 7.06 (m, 2H), 6.79 (m, 2H), 4.78 (m, 3H), 3.68 (s, 3H), 1.79 (s, 3H). ^{13}C NMR (DMSO-d_6, δ): 172.6, 160.1, 158.0, 148.3, 138.0, 136.5, 129.1, 113.9, 103.4, 96.6, 65.3, 55.5, 34.2, 10.1. Anal. ($C_{16}H_{15}N_3O_3$) C, H, N.

3-Methyl-4-[4-(trifluoromethoxy)phenyl]-1,4,7,8-tetrahydro-5*H*-furo[3,4-*b*]pyrazolo[4,3-*e*]pyridin-5-one (16). ^{1}H NMR (DMSO-d_6, δ): 11.94 (s, 1H), 10.17 (s, 1H), 7.22−3.31 (m, 4H), 4.83 (m, 3H), 1.80 (s, 3H). ^{13}C NMR (DMSO-d_6, δ): 172.3, 160.6, 147.6, 147.1, 145.1, 136.7, 129.9, 121.2, 102.7, 96.0, 65.5, 34.5, 10.1. Anal. ($C_{16}H_{12}F_3N_3O_3$) C, H, N.

3-Methyl-4-[4-(methylsulfanyl)phenyl]-1,4,7,8-tetrahydro-5*H*-furo[3,4-*b*]pyrazolo[4,3-*e*]pyridin-5-one (17). ^{1}H NMR (DMSO-d_6, δ): 11.89 (s, 1H), 10.10 (s, 1H), 7.12 (bs, 4H), 4.80 (m, 3H), 2.41 (s, 3H), 1.81 (s, 3H). ^{13}C NMR (DMSO-d_6, δ): 172.6, 160.5, 147.7, 142.6, 137.0, 135.9, 128.8, 126.4, 103.1, 96.2, 65.4, 34.5, 15.4, 10.1. HRMS *m*/*z* (ESI) calcd for $C_{16}H_{16}N_3O_2S$ (M + H)$^+$, 314.0963; found, 314.0966.

3-Methyl-4-phenyl-1,4,7,8-tetrahydro-5*H*-furo[3,4-*b*]pyrazolo-[4,3-*e*]pyridin-5-one (18). ^{1}H NMR (DMSO-d_6, δ): 11.88 (s, 1H), 10.10 (s, 1H), 7.15−7.24 (m, 5H), 4.81 (m, 3H), 1.79 (s, 3H); ^{13}C NMR (DMSO-d_6, δ): 172.6, 160.4, 147.6, 145.8, 136.6, 128.6, 128.2, 126.6, 103.1, 96.4, 65.4, 35.1, 10.1. Anal. ($C_{15}H_{13}N_3O_2$) C, H, N.

3-Methyl-4-(2-nitrophenyl)-1,4,7,8-tetrahydro-5*H*-furo[3,4-*b*]-pyrazolo[4,3-*e*]pyridin-5-one (19). ^{1}H NMR (DMSO-d_6, δ): 12.02 (s, 1H), 10.25 (s, 1H), 7.24−7.80 (m, 4H), 5.47 (s, 1H), 4.79 (s, 2H), 1.80 (s, 3H). ^{13}C NMR (DMSO-d_6, δ): 172.3, 160.3, 149.2, 148.2, 136.9, 133.7, 132.2, 128.0, 123.9, 101.7, 95.5, 65.6, 29.6, 9.9. HRMS *m*/*z* (ESI) calcd for $C_{15}H_{12}N_4O_4Na$ (M + Na)$^+$, 335.0758; found, 335.0756.

4-(4-Hydroxy-3-methoxy-5-nitrophenyl)-3-methyl-1,4,7,8-tetrahydro-5*H*-furo[3,4-*b*]pyrazolo[4,3-*e*]pyridin-5-one (20). ^{1}H NMR (DMSO-d_6, δ): 11.97 (s, 1H), 10.17 (s, 1H), 7.22 (s, 1H), 7.13 (s, 1H), 4.81 (m, 3H), 3.82 (s, 3H), 1.87 (s, 3H). ^{13}C NMR (DMSO-d_6, δ): 172.7, 160.8, 149.6, 141.6, 137.0, 136.9, 136.5, 116.8, 114.7, 102.1, 95.5, 65.5, 57.1, 34.3, 10.1. Anal. ($C_{16}H_{14}N_4O_6$) C, H, N.

4-(3-Bromophenyl)-3-methyl-1,4,7,8-tetrahydro-5*H*-furo[3,4-*b*]pyrazolo[4,3-*e*]pyridin-5-one (21). ^{1}H NMR (DMSO-d_6, δ): 11.98 (s, 1H), 10.21 (s, 1H), 7.19−7.37 (m, 4H), 4.6 (m, 3H), 1.83 (s, 3H). ^{13}C NMR (DMSO-d_6, δ): 172.5, 160.7, 148.5, 147.5, 136.8, 130.9, 129.6, 127.4, 122.1, 102.5, 95.7, 65.5, 39.5, 10.1. Anal. ($C_{15}H_{12}BrN_3O_2$) C, H, N.

4-(3,5-Dibromo-4-hydroxyphenyl)-3-methyl-1,4,7,8-tetrahydro-5*H*-furo[3,4-*b*]pyrazolo[4,3-*e*]pyridin-5-one (22). ^{1}H NMR (DMSO-d_6, δ): 11.96 (s, 1H), 10.18 (s, 1H), 7.16−7.29 (m, 3H), 4.85 (m, 3H), 1.82 (s, 3H). ^{13}C NMR (DMSO-d_6, δ): 172.5, 160.7, 148.2, 147.5, 136.7, 133.3, 130.5, 128.0, 127.0, 126.7, 102.5, 95.7, 65.5, 34.8, 10.1. Anal. ($C_{15}H_{11}Br_2N_3O_3$) C, H, N.

4-(3-Bromo-4-ethoxy-5-methoxyphenyl)-3-methyl-1,4,7,8-tetrahydro-5*H*-furo[3,4-*b*]pyrazolo[4,3-*e*]pyridin-5-one (23). ^{1}H NMR (DMSO-d_6, δ): 11.96 (s, 1H), 10.16 (s, 1H), 6.97(s, 1H), 6.82 (s, 1H), 4.86 (m, 3H), 3.86 (q, J = 7.1 Hz, 2H), 3.76 (s, 3H), 1.88 (s, 3H), 1.27 (t, J = 6.9 Hz, 3H). ^{13}C NMR (DMSO-d_6, δ): 172.8, 160.8, 153.5,147.9, 143.7, 143.1, 136.8, 123.3, 117.5, 112.7, 102.5, 95.7, 68.9, 65.5, 56.6, 34.6, 16.0, 10.2. Anal. ($C_{18}H_{18}BrN_3O_4$) C, H, N.

2-Bromo-6-methoxy-4-(3-methyl-5-oxo-4,5,7,8-tetrahydro-1*H*-furo[3,4-*b*]pyrazolo[4,3-*e*]pyridin-4-yl)phenyl acetate (24). ^{1}H NMR (DMSO-d_6, δ): 12.00 (s, 1H), 10.20 (s, 1H), 7.07 (s, 1H), 6.91 (s, 1H), 4.87 (m, 3H), 3.75 (s, 3H), 2.29 (s, 3H), 1.90 (s, 3H). ^{13}C NMR (DMSO-d_6, δ): 172.6, 168.2, 160.9, 152.2, 147.5, 145.8, 136.8, 135.8, 123.1, 116.6, 112.3, 102.2, 95.5, 65.5, 56.8, 34.7, 20.7, 10.3. Anal. ($C_{18}H_{16}BrN_3O_5$) C, H, N.

4-[3-Bromo-4-(dimethylamino)phenyl]-3-methyl-1,4,7,8-tetrahydro-5*H*-furo[3,4-*b*]pyrazolo[4,3-*e*]pyridin-5-one (25). ^{1}H NMR (DMSO-d_6, δ): 11.95 (s, 1H), 10.14 (s, 1H), 7.07−7.31 (m, 3H), 4.85 (m, 3H), 2.65 (s, 6H), 1.85 (s, 3H). ^{13}C NMR (DMSO-d_6, δ): 172.6, 160.5, 150.0, 147.7, 141.8, 136.5, 132.9, 128.2, 121.1, 118.7, 102.7, 96.0, 65.4, 44.4, 33.9, 10.2. Anal. ($C_{17}H_{17}BrN_4O_2$) C, H, N.

4-(3-Bromo-4,5-dimethoxyphenyl)-3-methyl-1,4,7,8-tetrahydro-5*H*-furo[3,4-*b*]pyrazolo[4,3-*e*]pyridin-5-one (26). ^{1}H NMR (DMSO-d_6, δ): 11.93 (s, 1H), 10.13 (s, 1H), 6.98 (s, 1H), 6.83 (s, 1H), 4.87 (m, 3H), 3.78 (s, 3H), 3.69 (s, 3H), 1.89 (s, 3H). ^{13}C NMR (DMSO-d_6, δ): 172.3, 160.7, 153.5, 147.2, 144.4, 143.3, 136.8, 123.4, 116.9, 112.8, 102.4, 95.7, 65.5, 60.5, 56.6, 34.6, 10.2. HRMS *m*/*z* (ESI) calcd for $C_{17}H_{16}BrN_3O_4Na$ (M + Na)$^+$, 428.0214; found, 428.0222.

4-(3-Chlorophenyl)-3-methyl-1,4,7,8-tetrahydro-5*H*-furo[3,4-*b*]pyrazolo[4,3-*e*]pyridin-5-one (27). ^{1}H NMR (DMSO-d_6, δ): 11.96 (s, 1H), 10.18 (s, 1H), 7.16−7.29 (m, 3H), 4.85 (m, 3H), 1.82 (s, 3H). ^{13}C NMR (DMSO-d_6, δ): 172.5, 160.7, 148.2, 147.5, 136.7, 133.3, 130.5, 128.0, 127.0, 126.7, 102.5, 95.7, 65.5, 34.8, 10.1. Anal. ($C_{15}H_{12}ClN_3O_2$) C, H, N.

4-(3,4-Dichlorophenyl)-3-methyl-1,4,7,8-tetrahydro-5*H*-furo[3,4-*b*]pyrazolo[4,3-*e*]pyridin-5-one (28). ^{1}H NMR (DMSO-d_6, δ): 11.98 (s, 1H), 10.21 (s, 1H), 7.17−7.53 (m, 3H), 4.83 (m, 3H), 1.82 (s, 3H). ^{13}C NMR (DMSO-d_6, δ): 172.5, 160.8, 147.5, 146.8, 136.9, 131.2, 130.9, 130.1, 129.2, 128.7, 102.1, 95.4, 65.6, 34.3, 10.1. Anal. ($C_{15}H_{11}Cl_2N_3O_2$) C, H, N.

4-(3-Fluorophenyl)-3-methyl-1,4,7,8-tetrahydro-5*H*-furo[3,4-*b*]pyrazolo[4,3-*e*]pyridin-5-one (29). ^{1}H NMR (DMSO-d_6, δ): 11.96 (s, 1H), 10.18 (s, 1H), 6.97−7.33 (m, 4H), 4.85 (m, 3H), 1.83 (s, 3H). ^{13}C NMR (DMSO-d_6, δ): 172.7, 160.7, 149.0, 147.4, 136.8, 130.5, 130.4, 124.3, 114.7, 113.6, 113.3, 102.5, 95.7, 65.5, 34.8, 10.1. Anal. ($C_{15}H_{12}FN_3O_2$) C, H, N.

4-(2-Bromophenyl)-3-methyl-1,4,7,8-tetrahydro-5*H*-furo[3,4-*b*]pyrazolo[4,3-*e*]pyridin-5-one (30). ^{1}H NMR (DMSO-d_6, δ): 11.92 (s, 1H), 10.21 (s, 1H), 7.06−7.53 (m, 4H), 5.26 (s, 1H), 4.83 (s, 2H), 1.78 (s, 3H). ^{13}C NMR (DMSO-d_6, δ): 172.2, 160.9, 147.8, 136.5, 128.7, 122.8, 65.5, 10.1. Anal. ($C_{15}H_{12}BrN_3O_2$) C, H, N.

4-(4-Bromophenyl)-3-methyl-1,4,7,8-tetrahydro-5*H*-furo[3,4-*b*]pyrazolo[4,3-*e*]pyridin-5-one (31). ^{1}H NMR (DMSO-d_6, δ): 11.96 (s, 1H), 10.18 (s, 1H), 7.12−7.55 (m, 4H), 4.83 (m, 3H), 1.82 (s, 3H). ^{13}C NMR (DMSO-d_6, δ): 172.5, 160.6, 147.5, 145.1, 136.7, 131.5, 130.5, 119.7, 102.6, 95.9, 65.5, 34.6, 10.1. Anal. ($C_{15}H_{12}BrN_3O_2$) C, H, N.

3,4-Dimethyl-1,4,7,8-tetrahydro-5*H*-furo[3,4-*b*]pyrazolo[4,3-*e*]pyridin-5-one (32). ^{1}H NMR (DMSO-d_6, δ): 11.83 (s, 1H), 9.86 (s, 1H), 4.73 (m, 3H), 2.14 (s, 3H), 1.23 (d, 3H). ^{13}C NMR (DMSO-d_6, δ): 173.2, 160.2, 147.5, 136.2, 104.1, 97.2, 65.3, 23.7, 22.4, 10.3. Anal. ($C_{10}H_{11}N_3O_2$) C, H, N.

3-Methyl-4-[(4*S*)-4-(1-methylethenyl)cyclohex-1-en-1-yl]-1,4,7,8-tetrahydro-5*H*-furo[3,4-*b*]pyrazolo[4,3-*e*]pyridin-5-one (33). ^{1}H NMR (DMSO-d_6, δ): 11.84 (s, 1H), 9.90 (s, 1H), 5.59 (s, 1H), 4.74 (m, 5H), 4.26 (s, 1H), 1.66−2.02 (m, 12H). ^{13}C NMR (DMSO-d_6, δ): 172.8, 161.2, 149.8, 148.1, 138.4, 136.5, 122.1, 121.6, 121.3, 109.5, 101.0, 100.6, 94.4, 94.0, 65.1, 37.3, 30.6, 27.8, 25.3, 21.2, 10.1. Anal. ($C_{18}H_{21}N_3O_2$) C, H, N.

4-(5-Chloro-3-methyl-1-phenyl-1*H*-pyrazol-4-yl)-3-methyl-1,4,7,8-tetrahydro-5*H*-furo[3,4-*b*]pyrazolo[4,3-*e*]pyridin-5-one (34). ^{1}H NMR (DMSO-d_6, δ): 11.94 (s, 1H), 10.18 (s, 1H), 7.42−7.49 (m, 5H), 4.84 (m, 3H), 1.98 (s, 3H), 1.87 (s, 3H). ^{13}C NMR (DMSO-d_6, δ): 172.4, 160.8, 148.3, 138.5, 136.6, 129.7, 128.4, 125.0, 124.9, 120.0, 100.7, 93.6, 65.4, 24.5, 12.9, 9.8. Anal. ($C_{19}H_{16}ClN_5O_2$) C, H, N: calcd, 59.77, 4.22, 18.34; found, 59.17, 4.25, 17.96.

3-Methyl-4-thiophen-2-yl-1,4,7,8-tetrahydro-5*H*-furo[3,4-*b*]-pyrazolo[4,3-*e*]pyridin-5-one (35). ^{1}H NMR (DMSO-d_6, δ): 11.97 (s, 1H), 10.16 (s, 1H), 6.87−7.25 (m, 3H), 5.19 (s, 1H), 4.79 (s, 2H), 1.94 (s, 3H). ^{13}C NMR (DMSO-d_6, δ): 172.4, 160.0, 150.7, 147.4, 137.0, 127.0, 124.6, 124.2, 102.8, 96.1, 65.3, 30.0, 10.1. HRMS *m*/*z* (ESI) calcd for $C_{13}H_{12}N_3O_2S$ $(M + H)^+$, 314.0650; found, 314.0663.

3-Methyl-4-thiophen-3-yl-1,4,7,8-tetrahydro-5*H*-furo[3,4-*b*]-pyrazolo[4,3-*e*]pyridin-5-one (36). ^{1}H NMR (DMSO-d_6, δ): 11.91 (s, 1H), 10.10 (s, 1H), 6.89−7.36 (m, 3H), 4.79 (m, 3H), 1.90 (s, 3H). ^{13}C NMR (DMSO-d_6, δ): 172.7, 160.3, 147.4, 146.5, 136.7, 128.0, 126.2, 121.0, 102.5, 96.0, 65.3, 30.0, 10.09. HRMS *m*/*z* (ESI) calcd for $C_{13}H_{12}N_3O_2S$ $(M + H)^+$, 314.0650; found, 314.0654.

3-Methyl-4-pyridin-4-yl-1,4,7,8-tetrahydro-5*H*-furo[3,4-*b*]-pyrazolo[4,3-*e*]pyridin-5-one (37). ^{1}H NMR (DMSO-d_6, δ): 11.98 (s, 1H), 10.22 (s, 1H), 8.46 (s, 2H), 7.23 (s, 2H), 4.86 (m, 3H), 1.84 (s, 3H). ^{13}C NMR (DMSO-d_6, δ): 172.4, 161.0, 154.0, 149.8, 147.5, 136.9, 123.7, 101.6, 95.0, 65.6, 34.6, 10.1. HRMS *m*/*z* (ESI) calcd for $C_{14}H_{13}N_4O_2$ $(M + H)^+$, 269.1038; found, 269.1039.

3-Methyl-4-pyridin-3-yl-1,4,7,8-tetrahydro-5*H*-furo[3,4-*b*]-pyrazolo[4,3-*e*]pyridin-5-one (38). ^{1}H NMR (DMSO-d_6, δ): 11.97 (s, 1H), 10.20 (s, 1H), 8.21 (m, 2H), 7.52 (s, 1H), 7.29 (s, 1H), 4.85 (m, 3H), 1.80 (s, 3H). ^{13}C NMR (DMSO-d_6, δ): 172.5, 160.9, 149.4, 147.9, 141.0, 135.8, 124.1, 102.3, 95.4, 65.5, 32.6, 10.0. HRMS *m*/*z* (ESI) calcd for $C_{14}H_{13}N_4O_2$ $(M + H)^+$, 269.1038; found, 269.1039.

3-Methyl-4-(6-methylimidazo[2,1-*b*][1,3]thiazol-5-yl)-1,4,7,8-tetrahydro-5*H*-furo[3,4-*b*]pyrazolo[4,3-*e*]pyridin-5-one (39). ^{1}H NMR (DMSO-d_6, δ): 12.00 (s, 1H), 10.31 (s, 1H), 7.07 (s, 2H), 5.26 (s, 1H), 4.84 (m, 2H), 2.20 (s, 3H), 1.77 (s, 3H). ^{13}C NMR (DMSO-d_6, δ): 172.2, 161.0, 147.8, 146.8, 139.3, 136.9, 124.2, 118.2, 112.4, 99.8, 93.0, 65.4, 65.5, 25.1, 13.9, 9.6. HRMS *m*/*z* (ESI) calcd for $C_{15}H_{14}N_5O_2S$ $(M + H)^+$, 328.0868; found, 328.0875.

3-Methyl-4-(3-methylquinoxalin-2-yl)-1,4,7,8-tetrahydro-5*H*-furo[3,4-*b*]pyrazolo[4,3-*e*]pyridin-5-one (40). ^{1}H NMR (DMSO-d_6, δ): 11.95 (s, 1H), 10.30 (s, 1H), 7.72−7.96 (m, 4H), 5.49 (s, 1H), 4.92 (m, 2H), 2.68 (s, 3H), 1.64 (s, 3H). ^{13}C NMR (DMSO-d_6, δ): 172.6, 161.3, 157.3, 153.3, 147.9, 140.9, 136.7, 130.1, 129.7, 129.0, 128.5, 101.0, 94.4, 65.8, 36.4, 23.2, 9.9. Anal. ($C_{18}H_{15}N_5O_2$) C, H, N.

Cell Culture. Human T-cell leukemia cell line Jurkat (ATCC TIB-152, E6−1 clone) and human cervical cancer cell line HeLa (ATCC S3) were cultured in RPMI-1640 (Gibco) and supplemented with 10% FBS (Gibco), 100 mg/L penicillin G, 100 mg/L streptomycin, 1.0 mM sodium pyruvate, 1.5 g/L sodium bicarbonate, and 4.5 g/L glucose (all from Sigma) at 37 °C in a humidified atmosphere with 10% CO_2. MCF-7/AZ, a variant of the human mammary carcinoma cells MCF-7, were cultured in a mixture of DMEM and HAMF12 (50/50) (Invitrogen) supplemented with 250 IU/mL penicillin, 100 μg/mL streptomycin, and 10% FBS.

Primary Lymphocytes. A 10 mL sample of whole blood was collected from healthy donors (DHHS # FWA 00006606) into a syringe containing 10 μL of heparin (5U/ul, Elkins-Sinn, Inc., Cherry Hill, NJ). The leukocytes were isolated from the whole blood by centrifuging at 500 G in histopaque-1119 (Sigma Diagnostics, Inc., St. Louis, MO) solution for 30 min resulting in the formation of distinct layers of plasma, lymphocytes, neutrophils, and red blood cells. Leukocytes were carefully collected into 15 mL tubes, washed with HHB (30 mM HEPES, 110 mM NaCl, 10 mM KCl, 1 mM $MgCl_2$, and 10 mM glucose), then centrifuged at 400 G for 10 min. The supernatant was discarded, and the pellet was resuspended into media (RPMI-1640 and 10% FBS) and incubated similar to Jurkat cells (37 °C, 10% CO_2, and 95% humidity).

Annexin-V Apoptosis Assay. 2×10^5 Jurkat cells/mL were plated in 24 well plates and treated with 5 μM concentration of the compounds, 0.1% (v/v) DMSO, 5 μM **1**, and 50 μM **2** (both Fisher) in duplicates and incubated for 48 h. The cells were centrifuged at 400 G for 1 min. The supernatant was discarded, and the cells were resuspended in 100 μL per sample of Annexin-V−FITC/propidium iodide solution in HHB (3 μL of $CaCl_2$ (1.5 M) per mL HHB, 2 μL (10 mg/mL) of propidium iodide (Sigma) per mL HHB, and 20 μL of Annexin-V−FITC (Southern Biotech, Birmingham, AL) per mL HHB). The samples in the labeling solution were transferred into Falcon tubes and incubated in a water bath at 37 °C for 20 min. The samples were then analyzed using a Becton Dickinson FACscan flow cytometer with CellQuest software. The results were tabulated as percent of Annexin-V−FITC positive apoptotic cells.

DNA Laddering. Approximately 1×10^6 Jurkat cells were treated with compound **13** at 50 μM, 10 μM, 5 μM, and 1 μM concentrations along with 0.1% DMSO and 50 μM **2** as controls for 24 h. Cells were collected and centrifuged at 400 G for 1 min. The supernatant was discarded, and the cells were gently resuspended in 20 μL of lysis buffer (50 mM Tris-HCL, pH 8, 10 mM EDTA, 0.5% SDS and 0.5 mg/mL proteinase K (Sigma)) over ice. The suspension of lysed cells was first incubated at 55 °C for 60 min, and then 5 μL of RNase (Sigma) was added and incubated at 55 °C for another 60 min. The debris was collected by centrifugation, and the supernatant was collected. The lysate was heated to 70 °C, and loading buffer (20 μL of TE buffer (10 mM Tris-HCl, 1 mM EDTA) and 10 μL of FOG) was added. The samples were loaded on a 1.5% agarose gel containing 0.5 μg/mL ethidium bromide and were run at 80 V for approximately 1 h and visualized under UV light.

MTT Assay. Cells were transferred to microtiter plates in 100 μL of medium at a concentration of 2×10^4 cells/mL. HeLa and MCF-7/AZ cells were incubated for 24 h before treating with the drugs to allow proper adhesion while Jurkat cells were treated immediately. Cells were treated with the panel of the test compounds and incubated for 48 h. 20 μL of MTT reagent (5 mg/

mL) was added to each well and incubated further for 2 h. The resulting formazan crystals were dissolved in 100 μL of DMSO, and the OD was determined at a wavelength of 490 nm.[35] The experiments were repeated at least three times for each compound per cell line.

Caspase-3 Activity Assay. Caspase-3 activation was detected by using a Caspase-3 colorimetric activity assay kit (Chemicon, Temecula, CA), which assays the activity of caspase-3, recognizing the sequence DEVD. The assay is based on spectrophotometric detection of *p*-nitroaniline (*p*NA) after cleavage of the labeled substrate DVED-*p*-NA. Therefore, Jurkat cells were treated with a panel of test compounds (5 μM), and controls included cells treated with DMSO, **1** (5 μM), COL (5 μM), and VIN (1 μM). 1×10^6 cells were harvested and lysed with lysis buffer. Protein concentration of each sample was determined using Pierce BCA protein assay kit (Pierce, Rockford, IL). Each sample was mixed with caspase-3 substrate (DEVD-*p*-nitroaniline) and incubated at 37 °C for 2 h in 96 well plates (LPS, Rochester, NY). Samples were read at 405 nm using a spectrophotometer (Molecular Devices, CA).

Western Blot Analysis. The ability of compound **13** to induce caspase-3 activity and to cleave one of its main targets, PARP, was tested by treating Jurkat cells with the compound at a concentration of 5 μM for indicated hours. Control cultures were treated with DMSO, **1** (5 μM), VIN (1 μM), and compound **39** (5 μM). The cells were washed two times with PBS and subsequently lysed in 0.4 mL lysis buffer containing 1% Triton X-100, 1% NP-40, and the following inhibitors: aprotinin (10 μg/mL), leupeptin (10 μg/mL), PMSF (1.72 mM), NaF (100 mM), $NaVO_3$ (500 μM), and $Na_4P_2O_7$ (500 μg/mL). Protein concentration was determined using Pierce BCA protein assay kit (Pierce, Rockford, IL). Aliquots of lysates containing the same quantity of proteins were boiled for 5 min in SDS-PAGE sample buffer containing 5% β-mercaptoethanol, separated by SDS-PAGE (7.5 and 12% gels), and transferred to PVDF membranes (Immobilon-P) (Bio-Rad Laboratories, Hercules, CA). After transfer, membranes were incubated with anti-PARP and anti-caspase-3 antibodies followed by incubation with a secondary biotinylated antibody (1:1000) and developed by ECL (Vectastain ABC-AmP) detection kit (Vector Labs, Burlingame, CA). Membranes were imaged and analyzed on the BioChemi System and analysis software (UVP, Upland, CA).

Acknowledgment. This work is supported by the Russian Foundation for Basic Research (Grant 07-03-00577 to I.V.M.) and U.S. National Institutes of Health (Grants RR-16480 and CA-99957 to A.K.) under the BRIN/INBRE and AREA programs. A.K. thanks Professor Patrick S. Mariano for his invaluable advice with the manuscript. This article is dedicated to the memory of Professor Victor N. Knyazev.

Supporting Information Available: Elemental analysis data. This material is available free of charge via the Internet at http://pubs.acs.org.

References

(1) Newman, D. J.; Cragg, G. M.; Snader, K. M. Natural products as sources of new drugs over the period 1981−2002. *J. Nat. Prod*. **2003**, *66*, 1022−1037.
(2) Koehn, F. E.; Carter, G. T. The evolving role of natural products in drug discovery. *Nat. Rev. Drug Discovery* **2005**, *4*, 206−220.
(3) Arve, L.; Voigt, T.; Waldmann, H. Charting biological and chemical space: PSSC and SCONP as guiding principles for the development of compound collections based on natural product scaffolds. *QSAR Comb. Sci*. **2006**, *25*, 449−456.
(4) Breinbauer, R.; Vetter, I. R.; Waldmann, H. From protein domains to drug candidates: Natural products as guiding principles in the design and synthesis of compound libraries. *Angew. Chem., Int. Ed*. **2002**, *41*, 2879−2890.
(5) Tan, D. S. Current progress in natural product-like libraries for discovery screening. *Comb. Chem. High Throughput Screening* **2004**, *7*, 631−643.
(6) Boldi, A. M. Libraries from natural product-like scaffolds. *Curr. Opin. Chem. Biol*. **2004**, *8*, 281−286.
(7) Liao, Y.; Hu, Y.; Wu, J.; Zhu, Q.; Donovan, M.; Fathi, R.; Yang, Z. Diversity oriented synthesis and branching reaction pathway to generate natural product-like compounds. *Curr. Med. Chem*. **2003**, *10*, 2285−2316.
(8) Feher, M.; Schmidt, J. M. Property distributions: Differences between drugs, natural products, and molecules from combinatorial chemistry. *J. Chem. Inf. Comput. Sci*. **2003**, *43*, 218−227.
(9) Gerencsér, J.; Dormán, G.; Darvas, F. Meldrum's acid in multicomponent reactions: Applications to combinatorial and diversity-oriented synthesis. *QSAR Comb. Sci*. **2006**, 439−448.
(10) Ramón, D. J.; Miguel, Y. Asymmetric multicomponent reactions (AMCRs): The new frontier. *Angew. Chem., Int. Ed*. **2005**, *44*, 1602−1634.
(11) Orru, R. V. A.; de Greef, M. Recent advances in solution-phase multicomponent methodology for the synthesis of heterocyclic compounds. *Synthesis* **2003**, 1471−1499.
(12) Hulme, C.; Gore, V. Multicomponent reactions: Emerging chemistry in drug discovery. From xylocain to crixivan. *Curr. Med. Chem*. **2003**, *10*, 51−80.
(13) Ugi, I.; Heck, S. The multicomponent reactions and their libraries for natural and preparative chemistry. *Comb. Chem. High Throughput Screening* **2001**, *4*, 1−34.
(14) Weber, L.; Illgen, K.; Almstetter, M. Discovery of new multicomponent reactions with combinatorial methods. *Synlett* **1999**, 366−374.
(15) For a recent review, see: Kappe, C. O. The generation of dihydropyrimidine libraries utilizing Biginelli multicomponent chemistry. *QSAR Comb. Sci*. **2003**, *22*, 630−645.
(16) Beck, B.; Hess, S.; Dömling, A. One-pot synthesis and biological evaluation of aspergillamides and analogues. *Bioorg. Med. Chem. Lett*. **2000**, *10*, 1701−1705.
(17) For the synthesis of nikkomycin analogues utilizing the Ugi process on solid support, see: Suda, A.; Ohta, A.; Sudoh, M.; Tsukuda, T.; Shimma, N. Combinatorial synthesis of nikkomycin analogues on solid support. *Heterocycles* **2001**, **55**, 1023−1028.
(18) Imbert, T. F. Discovery of podophyllotoxins. *Biochimie* **1998**, *80*, 207−222.
(19) Bohlin, L.; Rosen, B. Podophyllotoxin derivatives: Drug discovery and development. *Drug Discovery Today* **1996**, *1*, 343−351.
(20) Long, B. H.; Minocha, A. Inhibition of Topoisomerase-II by Vp-16−213 (Etoposide), Vm-26 (Teniposide), and structural congeners as an explanation for in vivo DNA breakage and cytotoxicity. *Proc. Am. Assoc. Cancer Res.* **1983**, *24*, 321−321.
(21) You, Y. J. Podophyllotoxin derivatives: Current synthetic approaches for new anticancer agents. *Curr. Pharm. Des*. **2005**, *11*, 1695−1717.
(22) Gordaliza, M.; Castro, M. A.; Corral, J. M. M.; San Feliciano, A. Antitumor properties of podophyllotoxin and related compounds. *Curr. Pharm. Des*. **2000**, *6*, 1811−1839.
(23) Berkowitz, D. B.; Maeng, J. −H.; Dantzig, A. H.; Shepard, R. L.; Norman, B. H. Chemoenzymatic and ring E-modular approach to the (-)-podophyllotoxin skeleton. Synthesis of 3′,4′,5′-tridemethoxy-(-)-podophyllotoxin. *J. Am. Chem. Soc*. **1996**, *118*, 9426−9427.
(24) Hitotsuyanagi, Y.; Kobayashi, M.; Fukuyo, M.; Takeya, K.; Itokawa, H. A facile synthesis of the 4-aza-analogs of 1-arylnaphthalene lignans - Chinensin, justicidin B, and Taiwanin C. *Tetrahedron Lett.* **1997**, *38*, 8295−8296.
(25) Hitotsuyanagi, Y.; Fukuyo, M.; Tsuda, K.; Kobayashi, M.; Ozeki, A.; Itokawa, H.; Takeya, K. 4-Aza-2,3-dehydro-4-deoxypodophyllotoxins: Simple aza-podophyllotoxin analogues possessing potent cytotoxicity. *Bioorg. Med. Chem. Lett*. **2000**, *10*, 315−317.
(26) Gensler, W. J.; Murthy, C. D.; Trammell, M. H. Non-enolizable podophyllotoxin derivatives. *J. Med. Chem*. **1977**, *20*, 635−644.
(27) Tratrat, C.; Giorgi-Renault, S.; Husson, H. P. A multicomponent reaction for the one-pot synthesis of 4-aza-2,3-didehydropodophyllotoxin and derivatives. *Org. Lett*. **2002**, *4*, 3187−3189.
(28) Jardine, I. In *Anticancer Agents Based on Natural Products*; Cassady, J. M., Douros, J. D., Eds.; Academic: New York, 1980; pp 319−351.
(29) Ayres, D. C.; Loike, J. D. *Lignans, Chemical, Biological and Clinical Properties*; Cambridge University Press: Cambridge, 1990.
(30) Wright, J. L.; Gregory, T. F.; Kesten, S. R.; Boxer, P. A.; Serpa, K. A.; Meltzer, L. T.; Wise, L. D. Subtype-selective N-methyl-D-aspartate receptor antagonists: Synthesis and biological evaluation of 1-(heteroarylalkynyl)-4-benzylpiperidines. *J. Med. Chem*. **2000**, *43*, 3408−3419.
(31) Wilkening, R. R.; Ratcliffe, R. W.; Fried, A. K.; Meng, D.; Sun, W.; Colwell, L.; Lambert, S.; Greenlee, M.; Nilsson, S.; Thorsell, A.; Mojena, M.; Tudela, C.; Frisch, K.; Chan, W.; Birzin, E. T.; Rohrer, S. P.; Hammond, M. L. Estrogen receptor beta-subtype selective tetrahydrofluorenones: Use of a fused pyrazole as a phenol bioisostere. *Bioorg. Med. Chem. Lett*. **2006**, *16*, 3896−3901.

(32) For preliminary communication of this work, see: Magedov, I. V.; Manpadi, M.; Rozhkova, E.; Przheval'skii, N. M.; Rogelj, S.; Shors, S. T.; Steelant, W. F. A.; Van slambrouck, S.; Kornienko, A. Structural simplification of bioactive natural products with multicomponent synthesis: Dihydropyridopyrazole analogues of podophyllotoxin. *Bioorg. Med. Chem. Lett*. **2007**, *17*, 1381−1385.
(33) (a) Quiroga, J.; Insuasty, B.; Hormaza, A.; Saitz, C.; Jullian, C. Synthesis of 4-aryl-4,7,8,9-tetrahydro-6H-pyrazolo[3,4-b]quinolin-5-ones. *J. Heterocycl. Chem*. **1998**, *35*, 575−578.
(34) Quiroga, J.; Mejía, D.; Insuasty, B.; Abonía, R.; Nogueras, M.; Sánchez, A.; Cobo, J.; Low, J. N. Regioselective synthesis of 4,7,8,9-tetrahydro-2H-pyrazolo[3,4-b]-quinolin-5(6H)-ones. Mechanism and structural analysis. *Tetrahedron* **2001**, *57*, 6947−6953.
(35) Mosmann, T. Rapid colorimetric assay for cellular growth and survival - application to proliferation and cytotoxicity assays. *J. Immunol. Methods* **1983**, *65*, 55−63.
(36) Although the antiproliferative effect of the tested compounds is generally much higher at 50 μM, the direct comparison of these data is impeded by limited solubility of a number of these compounds at this concentration.
(37) Vermes, I.; Haanen, C.; Steffens-Nakken, H.; Reutelingsperger, C. A novel assay for apoptosis - flow cytometric detection of phosphatidylserine expression on early apoptotic cells using fluorescein-labeled annexin-V J. *Immunol. Methods* **1995**, *184*, 39−51.
(38) Fadok, V. A.; Voelkler, D. R.; Campbell, P. A.; Cohen, J. J.; Bratton, D. L.; Henson, P. M. Exposure of phosphatidylserine on the surface of apoptotic lymphocytes triggers specific recognition and removal by macrophages. *J. Immunol*. **1992**, *148*, 2207−2216.
(39) For example, see: Vial, J. P.; Belloc, F.; Dumain, P.; Besnard, S.; Lacombe, F.; Boisseau, M. R.; Reiffers, J.; Bernard, P. Study of the apoptosis induced in vitro by antitumoral drugs on leukaemic cells. *Leuk. Res*. **1997**, *21*, 163−172.
(40) Zhang, H. −Z.; Kasibhatla, S.; Kuemmerle, J.; Kemnitzer, W.; Ollis-Mason, K.; Qiu, L.; Crogan-Grundy, C.; Tseng, B.; Drewe, J.; Cai, S. X. Discovery and structure-activity relationship of 3-aryl-5-aryl-1,2,4-oxadiazoles as a new series of apoptosis inducers and potential anticancer agents. *J. Med. Chem*. **2005**, *48*, 5215−5223.
(41) Kemnitzer, W.; Kasibhatla, S.; Jiang, S.; Zhang, H.; Zhao, J.; Jia, S.; Xu, L.; Crogan-Grundy, C.; Denis, R.; Barriault, N.; Vaillancourt, L.; Charron, S.; Dodd, J.; Attardo, G.; Labrecque, D.; Lamothe, S.; Gourdeau, H.; Tseng, B.; Drewe, J.; Cai, S. X. Discovery of 4-aryl-4H-chromenes as a new series of apoptosis inducers using a cell- and caspase-based high-throughput screening assay. 2. Structure−activity relationships of the 7- and 5-, 6-, 8-positions. *Bioorg. Med. Chem. Lett*. **2005**, *15*, 4745−4751.
(42) Kemnitzer, W.; Drewe, J.; Jiang, S.; Zhang, H.; Wang, Y.; Zhao, J.; Jia, S.; Herich, J.; Labreque, D.; Storer, R.; Meerovitch, K.; Bouffard, D.; Rej, R.; Denis, R.; Blais, C.; Lamothe, S.; Attardo, G.; Gourdeau, H.; Tseng, B.; Kasibhatla, S.; Cai, S. X. Discovery of 4-aryl-4H-chromenes as a new series of apoptosis inducers using a cell- and caspase-based high-throughput screening assay. 1. Structure-activity relationships of the 4aryl group. *J. Med. Chem*. **2004**, *47*, 6299−6310.

JM070528F